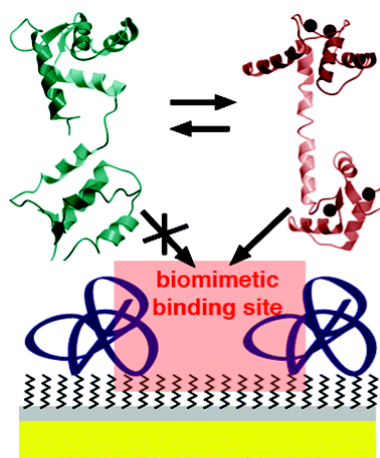


- Biomimetic Conformation-Specific Assembly of Proteins at Artificial Binding Sites Nanopatterned on Silicon

1

de la Rica, R.; Matsui, H. *J. Am. Chem. Soc.* **2009**, *131*, 14180–14181.

Abstract:

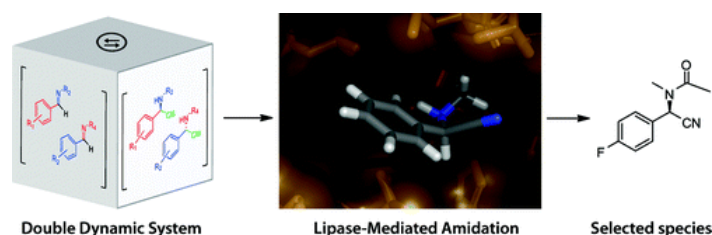


Biomolecules such as enzymes and antibodies possess binding sites where the molecular architecture and the physicochemical properties are optimum for their interaction with a particular target, in some cases even differentiating between stereoisomers. Here, we mimic this exquisite specificity via the creation of a suitable chemical environment by fabricating artificial binding sites for the protein calmodulin (CaM). By downscaling well-known surface chemical modification methodologies to the nanometer scale via silicon nanopatterning, the  $\text{Ca}^{2+}$ -CaM conformer was found to selectively bind the biomimetic binding sites. The methodology could be adapted to mimic other protein-receptor interactions for sensing and catalysis.

- Dynamic Asymmetric Multicomponent Resolution: Lipase-Mediated Amidation of a Double Dynamic Covalent System

Vongvilai, P.; Ramström, O. *J. Am. Chem. Soc.* **2009**, *131*, 14419–14425.

Abstract:

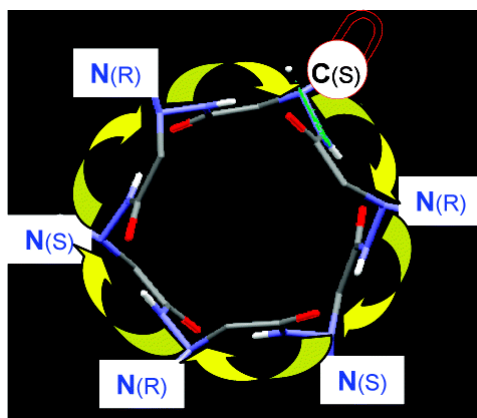


The Strecker reaction is one of the most important multicomponent reactions developed, leading to  $\alpha$ -aminonitriles that are versatile substrates for many synthetic applications. In the present study, this reaction type has been applied to a double dynamic covalent resolution protocol, leading to efficient C–C- and C–N-bond generation as well as chiral discrimination. The combination of transimination with imine-cyanation enabled the dynamic exchange in more than one direction around a single stereogenic center of restricted structure. This multiple exchange process could generate a vast range of compounds from a low number of starting materials in very short time. The resulting double dynamic covalent systems, created under thermodynamic control, were subsequently coupled in a one-pot process with kinetically controlled lipase-mediated transacylation. This resulted in complete resolution of the dynamic systems, yielding the optimal *N*-acyl- $\alpha$ -

aminonitriles for the enzyme, where the individual chemoenzymatic reactions could produce enantiomerically pure acylated *N*-substituted  $\alpha$ -aminonitriles in good yields.

- Aza- $\beta^3$ -cyclopeptides: A New Way of Controlling Nitrogen Chirality  
Mocquet, C.; Salaün, A.; Claudon, P.; Le Grel, B.; Potel, M.; Guichard, G.; Jamart-Grégoire, B.; Le Grel, P. *J. Am. Chem. Soc.* **2009**, *131*, 14521–14525.

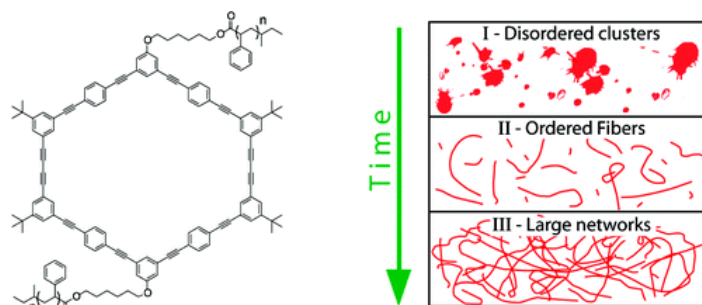
Abstract:



Sixteen and 24 membered aza- $\beta^3$ -peptidic macrocycles containing a  $\alpha$ -hydrazinoacid or a  $\beta^3$ -aminoacid were synthesized. The conformation of these pseudopeptides was determined by using NH chemical shift analysis, NH extinction, VT-NMR experiments, and X-ray diffraction. The study shows that a stable conformation is retained between 223 and 413 K. The latter is characterized by an uninterrupted internal H-bond network and a syndiotactic arrangement of the asymmetric centers. It means that the presence of the optically pure residue acts as a conformational lock to select a single enantiomer through the cyclization by controlling the absolute configuration of all the nitrogen atoms. To our knowledge, this represents the first example of a dynamic enantioselection process involving several centers prone to pyramidal inversion. These results give a new impulsion to the control of nitrogen chirality, which remained limited to small cycles for 60 years.

- Aggregation Kinetics of Macrocycles Detected by Magnetic Birefringence  
Gielen, J. C.; Heyen, A.; Klyatskaya, S.; Vanderlinden, W.; Höger, S.; Maan, J. C.; De Feyter, S.; Christianen, P. C. M. *J. Am. Chem. Soc.* **2009**, *131*, 14134–14135.

Abstract:



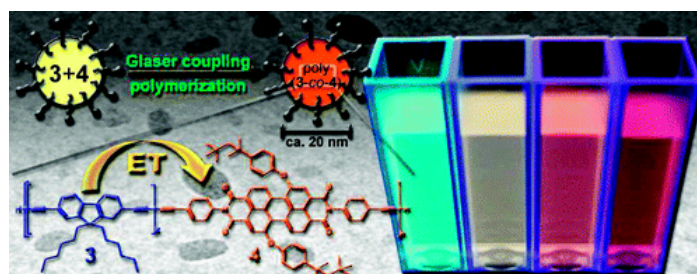
We have used magnetic-field-induced birefringence as a new sensitive technique to probe the aggregation kinetics of macrocyclic molecules in solution. We have found three consecutive aggregation stages: disordered objects, ordered fibers, and a network. The transition from disordered objects to ordered fibers is found to be slow, taking days or weeks to complete. We attribute this to the molecular tails of the macrocycles, which hamper fiber formation. We anticipate that linking

aggregation kinetics to molecular properties will lead to a better understanding of the mechanisms by which molecules self-assemble, allowing for a more rational design of the molecular building blocks.

3

- Fluorescent Conjugated Polymer Nanoparticles by Polymerization in Miniemulsion  
Baier, M. C.; Huber, J.; Mecking, S. *J. Am. Chem. Soc.* **2009**, *131*, 14267–14273.

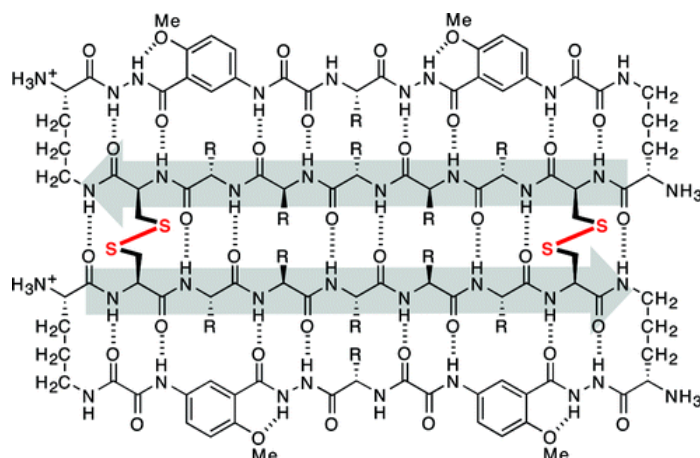
Abstract:



Highly fluorescent conjugated polymer nanoparticles were prepared directly by polymerization in aqueous miniemulsion, employing Glaser coupling polymerization as a suitable step-growth reaction. A 4,4'-dinonyl-2,2'-bipyridine-modified catalyst was found to be suited for the polymerization in the aqueous heterophase system. Nanoparticles of poly(arylene diethynylenes) (arylene = 2,5-dialkoxy phenylenes and 9,9'-dihexyl fluorene) with molecular weights in the range of  $M_n$  104 to 105 g mol<sup>-1</sup> and with sizes of  $\leq 30$  nm, as observed by TEM, result. N,N'-Di(4-ethynylphenyl)-1,7-di[4-(1,1,3,3-tetramethylbutyl)phenoxy]perylene-3,4:9,10-tetracarboxdiimide or 2,7-diethynylfluorenone was converted completely during the heterophase polymerization to afford colloidally stable nanoparticles of poly(arylene diethynylenes) with 0.1–2 mol % covalently incorporated perylene dye and 2–9 mol % of covalently incorporated fluorenone dye, respectively. Fluorescence spectroscopy of the aqueous dispersions reveals an efficient energy transfer to the dye in the nanoparticles, which enables a variation of the luminescence emission color between red ( $\lambda_{em}$  (max.) ca. 650 nm) and the green emission of the nanoparticles without dye.

- Use of Disulfide “Staples” To Stabilize  $\beta$ -Sheet Quaternary Structure  
Khakshoor, O.; Nowick, J. S. *Org. Lett.* **2009**, *11*, 3000–3003.

Abstract:



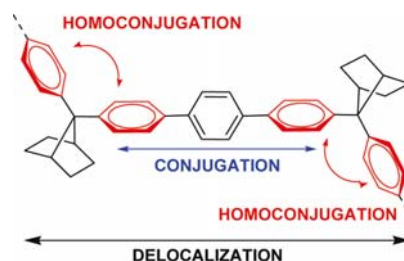
This Letter reports the use of disulfide linkages to stabilize a  $\beta$ -sheet dimer with a well-defined structure in aqueous and dimethyl sulfoxide solutions. In this dimer, two cyclic  $\beta$ -sheet peptides are connected by disulfide linkages at the non-hydrogen-bonded rings. The cyclic  $\beta$ -sheet “domains”

interact through hydrogen bonding to form a four-stranded  $\beta$ -sheet structure. This interaction results in enhanced folding of the cyclic  $\beta$ -sheet peptides.

- Efficient Electron Delocalization Mediated by Aromatic Homoconjugation in 7,7-Diphenylnorbornane Derivatives

Barcina, J. O.; del Rosario Colorado Heras, M.; Mba, M.; Gómez Aspe, R.; Herrero-García, N. J. *Org. Chem.* **2009**, *74*, 7148–7156.

Abstract:

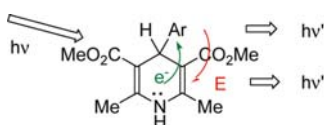


Efficient electron delocalization by aromatic homoconjugated 7,7-diphenylnorbornane (DPN) in alternated homoconjugated-conjugated block copolymers and reference compounds is revealed by photophysical and electrochemical measurements. The synthesis of the polymers was achieved by Suzuki polycondensation reaction. Effective electron delocalization by DPN is demonstrated by the significant red shifts observed in the absorption and emission spectra and the variation of the energy band gap of the polymers and monomeric model compounds in comparison to a series of oligophenylenes used as references (*p*-quaterphenyl, *p*-terphenyl, and biphenyl). The electron delocalization is also clearly demonstrated by the lower oxidation potential measured for homoconjugated model compound in comparison to *p*-terphenyl. The results show that the electron delocalization caused by two homoconjugated aryl rings is comparable to the effect produced by one conjugated aryl ring.

- Photoinduced Electron and Energy Transfer in Aryldihydropyridines

Jimenez, A. J.; Fagnoni, M.; Mella, M.; Albin, A. J. *Org. Chem.* **2009**, *74*, 6615–6622.

Abstract:



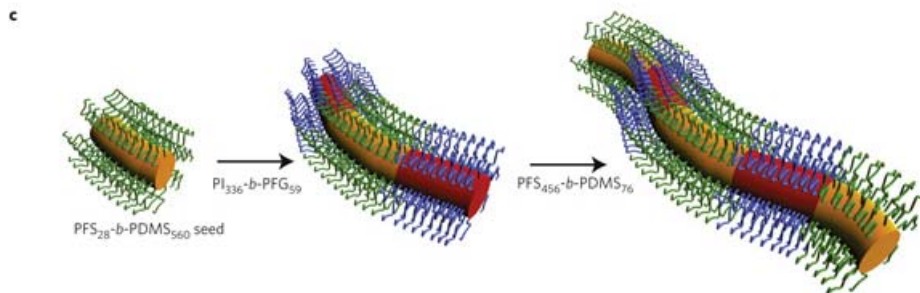
Dimethyl 2,6-dimethyl-1,4-dihydropyridine-3,5-dicarboxylates (Hantzsch DHPs) fluoresce weakly in fluid solution. However, these compounds exhibit an efficient fluorescence both in a viscous medium (glycerin) at room temperature and in a glassy matrix at 77 K (but no phosphorescence, since ISC is negligible). DHPs bearing an aryl group in position 4 have been synthesized. These contain two different  $\pi$  systems separated by an  $sp^3$  carbon (DHP-Ar dyads). The occurrence of energy and electron transfer processes between the chromophores is investigated through luminescence measurements. In particular, when  $^3Ar$  emits at a slow rate (e.g., Ar = phenanthryl) or not at all (Ar = nitrophenyl) the intradyad forward/backward electron transfer sequence offers a path for arriving at the DHP-localized triplet and the corresponding phosphorescence is observed. When  $^3Ar$  emits at a faster rate (Ar = acylphenyl), the phosphorescence from either of the two localized triplets,  $^3Ar$  or  $^3DHP$ , can be observed depending on  $\lambda_{exc}$ . When the aryl group has a triplet energy lower than that of  $^3DHP$ , this functions as emitting (4-cyano-1-naphthyl) or nonemitting ( $MeO_2CCH=CHC_6H_4$ ) energy

sink. The results document the possibility of building tailor-made Hantzsch aryldihydropyridines as versatile photoactivated dyads.

- Complex and hierarchical micelle architectures from diblock copolymers using living, crystallization-driven polymerizations

Gädt, T.; Jeong, N. S.; Cambridge, G.; Winnik, M. A.; Manners, I. *Nature Materials* **2009**, *8*, 144-150.

Abstract:

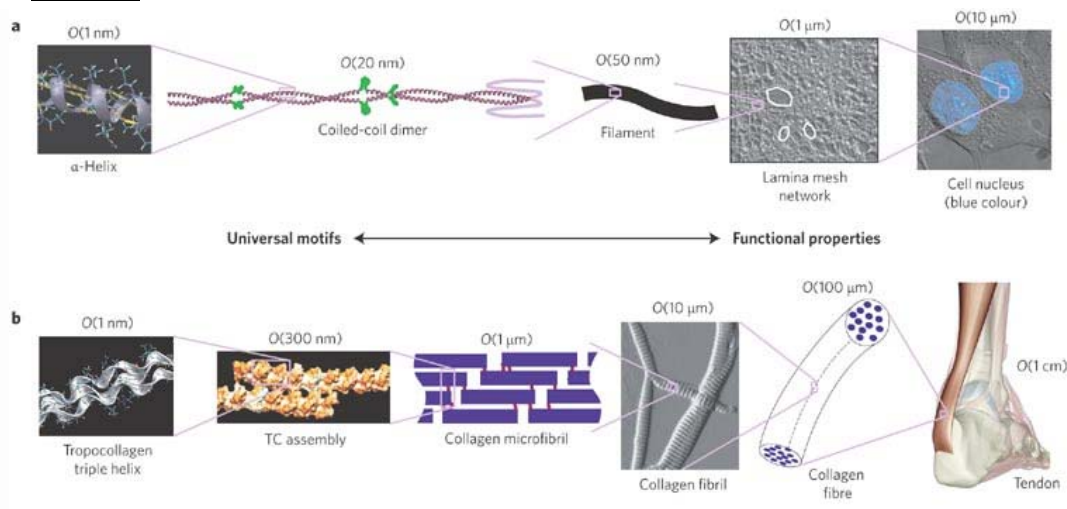


Block copolymers consist of two or more chemically distinct polymer segments, or blocks, connected by a covalent link. In a selective solvent for one of the blocks, core–corona micelle structures are formed. We demonstrate that living polymerizations driven by the epitaxial crystallization of a core-forming metalloblock represent a synthetic tool that can be used to generate complex and hierarchical micelle architectures from diblock copolymers. The use of platelet micelles as initiators enables the formation of scarf-like architectures in which cylindrical micelle tassels of controlled length are grown from specific crystal faces. A similar process enables the fabrication of brushes of cylindrical micelles on a crystalline homopolymer substrate. Living polymerizations driven by heteroepitaxial growth can also be accomplished and are illustrated by the formation of tri- and pentablock and scarf architectures with cylinder–cylinder and platelet–cylinder connections, respectively, that involve different core-forming metalloblocks.

- Deformation and failure of protein materials in physiologically extreme conditions and disease

Buehler, M. J.; Yung, Y. C. *Nature Materials* **2009**, *8*, 175-188.

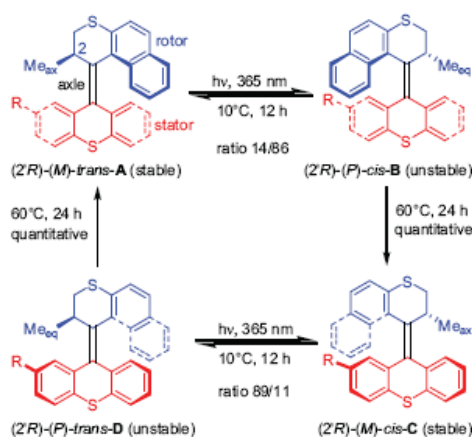
Abstract:



Biological protein materials feature hierarchical structures that make up a diverse range of physiological materials. The analysis of protein materials is an emerging field that uses the relationships between biological structures, processes and properties to probe deformation and failure phenomena at the molecular and microscopic level. Here we discuss how advanced experimental, computational and theoretical methods can be used to assess structure–process–property relations and to monitor and predict mechanisms associated with failure of protein materials. Case studies are presented to examine failure phenomena in the progression of disease. From this materials science perspective, a *de novo* basis for understanding biological processes can be used to develop new approaches for treating medical disorders. We highlight opportunities to use knowledge gained from the integration of multiple scales with physical, biological and chemical concepts for potential applications in materials design and nanotechnology.

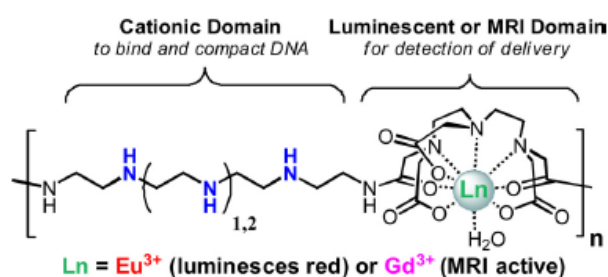
- Optimizing rotary processes in synthetic molecular motors  
Geertsema, E. M.; van der Molen, S. J.; Martens, M.; Feringa, B. L. *Proc. Nat. Acad. Sci.* **2009**, *106*, 16919–16924.

Abstract:



We deal with the issue of quantifying and optimizing the rotation dynamics of synthetic molecular motors. For this purpose, the continuous four-stage rotation behavior of a typical light-activated molecular motor was measured in detail. All reaction constants were determined empirically. Next, we developed a Markov model that describes the full motor dynamics mathematically. We derived expressions for a set of characteristic quantities, i.e., the average rate of quarter rotations or “velocity,”  $V$ , the spread in the average number of quarter rotations,  $D$ , and the dimensionless Péclet number,  $Pe = V/D$ . Furthermore, we determined the rate of full, four-step rotations ( $\Omega_{\text{eff}}$ ), from which we derived another dimensionless quantity, the “rotational excess,”  $r.e.$  This quantity, defined as the relative difference between total forward ( $\Omega_+$ ) and backward ( $\Omega_-$ ) full rotations, is a good measure of the unidirectionality of the rotation process. Our model provides a pragmatic tool to optimize motor performance. We demonstrate this by calculating  $V$ ,  $D$ ,  $Pe$ ,  $\Omega_{\text{eff}}$ , and  $r.e.$  for different rates of thermal versus photochemical energy input. We find that for a given light intensity, an optimal temperature range exists in which the motor exhibits excellent efficiency and unidirectional behavior, above or below which motor performance decreases.

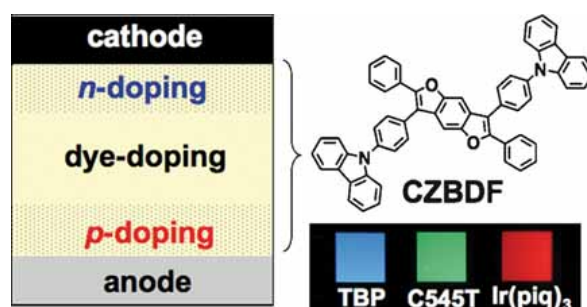
- Polymer beacons for luminescence and magnetic resonance imaging of DNA delivery  
Bryson, J. M.; Fichter, K. M.; Chu, W.-J.; Lee, J.-H.; Li, J.; Madsen, L. A.; McLendon, P. M.; Reineke, T. M. *Proc. Nat. Acad. Sci.* **2009**, *106*, 16913–16918.

Abstract:

The delivery of nucleic acids with polycations offers tremendous potential for developing highly specific treatments for various therapeutic targets. Although materials have been developed and studied for polynucleotide transfer, the biological mechanisms and fate of the synthetic vehicle has remained elusive due to the limitations with current labeling technologies. Here, we have developed polymer beacons that allow the delivery of nucleic acids to be visualized at different biological scales. The polycations have been designed to contain repeated oligoethylenamines, for binding and compacting nucleic acids into nanoparticles, and lanthanide (Ln) chelates [either luminescent europium ( $\text{Eu}^{3+}$ ) or paramagnetic gadolinium ( $\text{Gd}^{3+}$ )]. The chelated Lns allow the visualization of the delivery vehicle both on the nm/ $\mu\text{m}$  scale via microscopy and on the sub-mm scale via MRI. We demonstrate that these delivery beacons effectively bind and compact plasmid (p)DNA into nanoparticles and protect nucleic acids from nuclease damage. These delivery beacons efficiently deliver pDNA into cultured cells and do not exhibit toxicity. Micrographs of cultured cells exposed to the nanoparticle complexes formed with fluorescein-labeled pDNA and the europium-chelated polymers reveal effective intracellular imaging of the delivery process. MRI of bulk cells exposed to the complexes formulated with pDNA and the gadolinium-chelated structures show bright image contrast, allowing visualization of effective intracellular delivery on the tissue-scale. Because of their versatility, these delivery beacons possess remarkable potential for tracking and understanding nucleic acid transfer in vitro, and have promise as in vivo theranostic agents.

- Bis(carbazolyl)benzodifuran: A High-Mobility Ambipolar Material for Homo Junction Organic Light-Emitting Diode Devices

Tsuji, H.; Mitsui, C.; Sato, Y.; Nakamura, E. *Adv. Mater.* **2009**, 3776-3779.

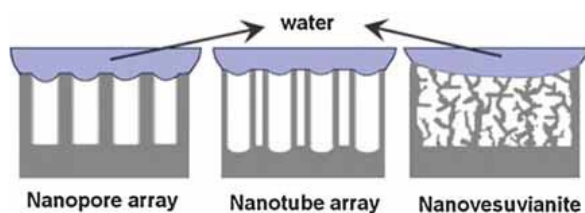
Abstract:

A new ambipolar material bis(carbazolyl)benzodifuran (CZBDF) shows well-balanced and high carrier mobilities for both holes and electrons ( $>10^{-3} \text{ cm}^2 \text{ V}^{-1} \text{ s}^{-1}$ ). This new material allows us to fabricate efficient *p-i-n* homo junction OLEDs that emit light across the full visible color range and perform at a level similar to state-of-the-art hetero junction devices.

- Designing Superhydrophobic Porous Nanostructures with Tunable Water Adhesion

Lai, Y.; Gao, X.; Zhuang, H.; Huang, J.; Lin, C.; Jiang, L. *Adv. Mater.* **2009**, 3799-3803.

Abstract:

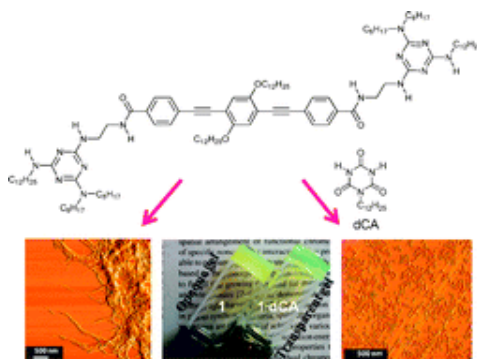


Basic principles of capillary-induced adhesion and roughness-enhanced hydrophobicity are utilized to design three superhydrophobic porous-nanostructure models whose adhesion forces ranged from strong to weak. The design idea is well-supported by experimental results, which indicated that adhesive forces may be tailored by modifying structural morphologies to manipulate solid-liquid contact behavior and air-pocket composition in open or sealed systems.

- Role of complementary H-bonding interaction of a cyanurate in the self-assembly and gelation of melamine linked tri(*p*-phenyleneethynylene)s.

Mahesh, S.; Thirumalai, R.; Yagai, S.; Kitamura, A.; Ajayaghosh, A. *Chem. Commun.* **2009**, 5984 – 5986.

Abstract:

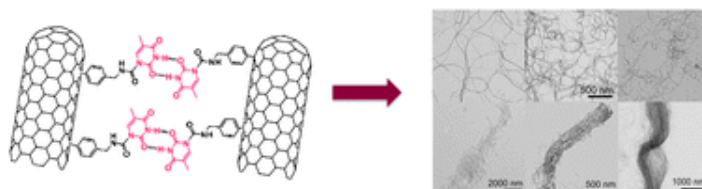


Melamine-functionalized tri(*p*-phenyleneethynylene) **1** self-assembles to form opaque and weak gels in aliphatic solvents which turned transparent and stable upon addition of a cyanurate, affording supramolecular nanostructures with distinct physical properties.

- Supramolecular aggregation of functionalized carbon nanotubes.

Quintana M.; Prato, M. *Chem. Commun.* **2009**, 6005 – 6007.

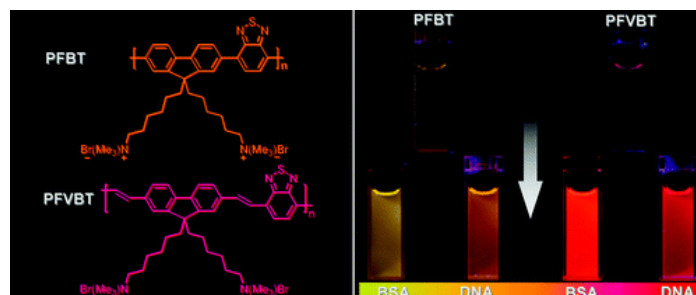
Abstract:



We describe the synthesis of novel carbon nanotubes functionalized with thymine units, able to induce self-assembly in a controlled supramolecular fashion.

- Design and Synthesis of Charge-Transfer-Based Conjugated Polyelectrolytes as Multicolor Light-Up Probes.

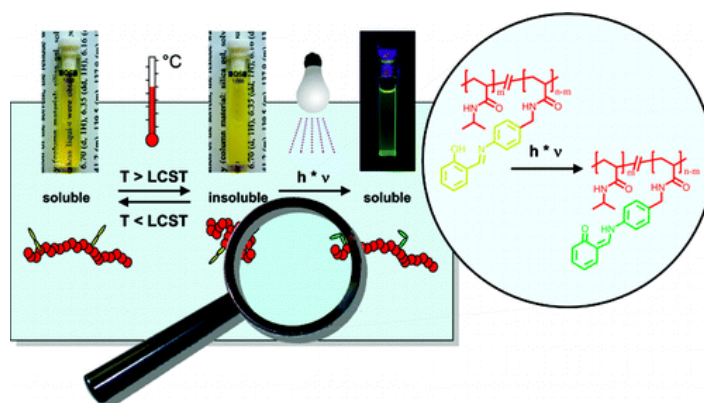
Pu, K.-Y.; Cai, L.; Liu, B. *Macromolecules* **2009**, 42, 5933–5940.

Abstract:

Cationic poly[9,9-bis(60-N,N,N-trimethylammonium)hexyl)fluorene-alt-4,7-(2,1,3-benzothiadiazole) dibromide] (PFBT) and poly[9,9-bis(60-(N,N,N-trimethylammonium)hexyl)fluorenyldivinylenealt-4,7-(2,1,3-benzothiadiazole)bromide] (PFVBT) are designed and synthesized to serve as multicolour light-up probes for biomolecular quantification. Because of the charge-transfer electronic states of the polymers, they exhibit weak fluorescence in aqueous media which can be significantly enhanced by increasing the hydrophobicity of polymeric microenvironment. Molecular orbital simulations further reveal that the presence of vinyl bonds endows PFVBT with a stronger charge-transfer character relative to that of PFBT. Both PFBT and PFVBT exhibit linear fluorescence enhancement as a function of bovine serum albumin (BSA) or DNA concentration in buffer solution, allowing effective biomolecular quantification. Of particular interest is that the light-up responses of PFBT or PFVBT in the presence of BSA and DNA are different, featuring biomolecule-dependent yellow-to-golden and orange-to-red light-up signatures, respectively. With a more sensitive light-up response, PFVBT can quantify biomolecules more effectively than PFBT does, which highlights the crucial role of charge transfer in determining the microenvironment-responsive fluorescence of conjugated polyelectrolytes for chemical and biological sensing.

- Temperature- and Light-Responsive Polyacrylamides Prepared by a Double Polymer Analogous Reaction of Activated Ester Polymers.

Jochum, F. D.; Theato, P. *Macromolecules* **2009**, *42*, 5941–5945.

Abstract:

Two different series of polyacrylamides containing different amounts of salicylideneaniline moieties have been synthesized via a double polymer analogous reaction of poly(pentafluorophenyl acrylate) (PPFPA). All copolymers were designed to exhibit a lower critical solution temperature (LCST) in aqueous solution, which was dependent on (i) the amount of incorporated chromophoric salicylideneaniline groups and (ii) the isomerization state of the respective salicylideneaniline group. Higher LCST values were measured for UV-irradiated solutions of the copolymers in comparison to the nonirradiated copolymer solutions. A maximum difference in the LCST of up to 13°C was found

for poly(*N*-cyclopropylacrylamide) copolymer containing 15.0 mol% of salicylidene aniline groups. Within this temperature range, a reversible solubility change of the copolymer could be induced by irradiation with light.

- New Pyrrole-Based Organic Dyes for Dye-Sensitized Solar Cells: Convenient Syntheses and High Efficiency

Li, Q.; Lu, L.; Zhong, C.; Huang, J.; Huang, Q.; Shi, J.; Jin, X.; Peng, T.; Qin, J.; Li, Z. *Chem. Eur. J.* **2009**, *15*, 9664-9668.

Abstract:

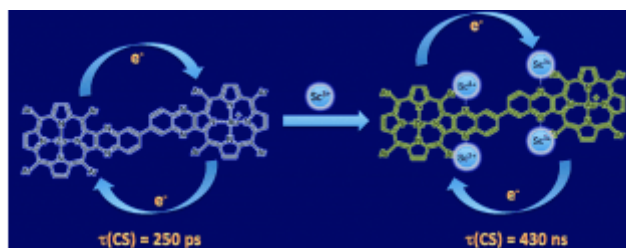


**Harvesting the sunshine:** Two new pyrrole-containing organic dyes were rationally designed and easily prepared. Thanks to the special electronic properties of pyrrole moieties and the introduction of the non-coplanar aromatic rings through a single bond (blue part in the above structure), a solar-cell device based on the sensitizer **LI-1** yields an overall conversion efficiency as high as 91 % of the standard cell from N719.

- Change in the Site of Electron-Transfer Reduction of a Zinc-Quinoxalinoporphyrin/Gold-Quinoxalinoporphyrin Dyad by Binding of Scandium Ions and the Resulting Remarkable Elongation of the Charge-Shifted-State Lifetime

Ohkubo, K.; Garcia, R.; Santic, P. J.; Khoury, T.; Crossley, M. J.; Kadish, K. M.; Fukuzumi, S. *Chem. Eur. J.* **2009**, *15*, 10493-10503.

Abstract:



**Long lifetime!** A dramatic effect of  $\text{Sc}^{3+}$  was observed on the electron-transfer reduction of gold(III) quinoxalino- and bisquinoxalinoporphyrins ( $\text{AuPQ}^+$  and  $\text{AuQPQ}^+$ ) (see figure), which not only changes the site of electron transfer from the  $\text{Au}^{\text{III}}$  metal to the fused quinoxaline part of the PQ macrocycle, but also leads to a remarkable elongation of the lifetime of the charge-shifted state of a ZnPQ-AuPQ dyad in benzonitrile. This is due to the strong binding of  $\text{Sc}^{3+}$  to the ZnPQ and  $\text{AuPQ}^+$  moieties.

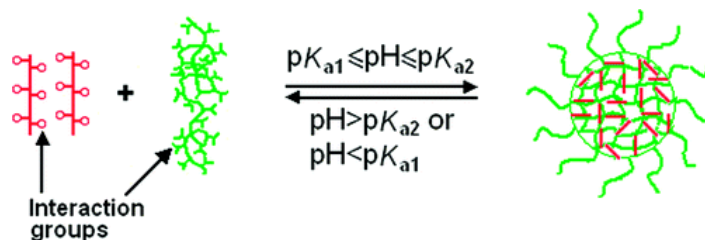
The site of electron-transfer reduction of  $\text{AuPQ}^+$  (PQ=5,10,15,20-tetrakis(3,5-di-*tert*-butylphenyl)quinoxalino[2,3-*b''*]porphyrin) and  $\text{AuQPQ}^+$  (QPQ=5,10,15,20-tetrakis(3,5-di-*tert*-butylphenyl)bisquinoxalino[2,3-*b''*:12,13-*b''''*]porphyrin) is changed from the  $\text{Au}^{\text{III}}$  center to the quinoxaline part of the PQ macrocycle in the presence of  $\text{Sc}^{3+}$  in benzonitrile because of strong binding of  $\text{Sc}^{3+}$  to the two nitrogen atoms of the quinoxaline moiety. Strong binding of  $\text{Sc}^{3+}$  to the corresponding nitrogen atoms on the quinoxaline unit of ZnPQ also occurs for the neutral form. The effects of  $\text{Sc}^{3+}$  on the photodynamics of an electron donor-acceptor compound containing a linked  $\text{Zn}^{\text{II}}$  and  $\text{Au}^{\text{III}}$  porphyrin ( $[\text{ZnPQ-AuPQ}]\text{PF}_6$ ) have been examined by femto- and nanosecond laser flash

photolysis measurements. The observed transient absorption bands at 630 and 670 nm after laser pulse irradiation in the absence of  $\text{Sc}^{3+}$  in benzonitrile are assigned to the charge-shifted (CS) state ( $\text{ZnPQ}^+-\text{AuPQ}$ ). The CS state decays through back electron transfer (BET) to the ground state rather than to the triplet excited state. The BET rate was determined from the disappearance of the absorption band due to the CS state. The decay of the CS state obeys first-order kinetics. The CS lifetime was determined to be 250 ps in benzonitrile. Addition of  $\text{Sc}^{3+}$  to a solution of  $\text{ZnPQ}-\text{AuPQ}^+$  in benzonitrile caused a drastic lengthening of the CS lifetime that was determined to be 430 ns, a value 1700 times longer than the 250 ps lifetime measured in the absence of  $\text{Sc}^{3+}$ . Such remarkable prolongation of the CS lifetime in the presence of  $\text{Sc}^{3+}$  results from a change in the site of electron transfer from the  $\text{Au}^{\text{III}}$  center to the quinoxaline part of the PQ macrocycle when  $\text{Sc}^{3+}$  binds to the quinoxaline moiety, which decelerate BET due to a large reorganization energy of electron transfer. The change in the site of electron transfer was confirmed by ESR measurements, redox potentials, and UV/Vis spectra of the singly reduced products.

- Stimuli-Sensitive Assemblies of Homopolymers

Sun, X.; Chen, T.; Huang, S.; Cai, F.; Chen, X.; Yang, Z.; Lu, Y.; Peng, H. *Langmuir* **2009**, *25*, 11980–11983.

Abstract:

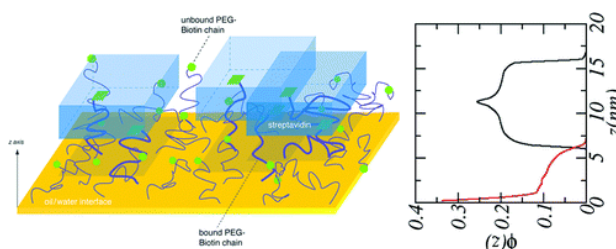


Two homopolymers assemble into nanoparticles in a common solvent of water through ionic complexation. These nanoparticles reversibly and rapidly respond to both pH and temperature, and are particularly promising as intelligent systems

- Streptavidin–Biotin Binding in the Presence of a Polymer Spacer. A Theoretical Description

Ren, C.-L.; Carvajal, D.; Shull, K. R.; Szleifer, I. *Langmuir* **2009**, *25*, 12283–12292.

Abstract:



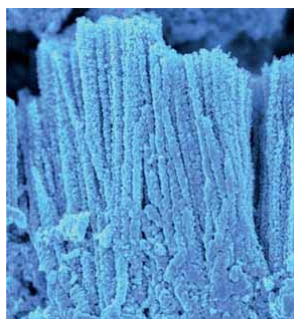
The binding of streptavidin to biotin located at the terminal ends of poly(ethylene oxide) tethered to a planar surface is studied using molecular theory. The theoretical model is applied to mimic experiments (Langmuir 2008, 24, 2472) performed using drop-shape analysis to study receptor-ligand binding at the oil/water interface. Our theoretical predictions show very good agreements with the experimental results. Furthermore, the theory enables us to study the thermodynamic and structural behavior of the PEO-biotin+streptavidin layer. The interfacial structure, shown by the volume fraction profiles of bound proteins and polymers, indicates that the proteins form a thick layer supported by stretched polymers, where the thickness of the layer is greater than the height of

the protein. When the polymer spacer is composed of PEO(3000), a thick layer with multilayers of proteins is formed, supported by the stretched polymer chains. It was found that thick multilayers of proteins are formed when long spacers are present or at very high protein surface coverages on short spacers. This shows that the flexibility of the polymer spacer plays an important role in determining the structure of the bound proteins due to their ability to accommodate highly distorted conformations to optimize binding and protein interactions. Protein domains are predicted when the amount of bound proteins is small due to the existence of streptavidin-streptavidin attractive interactions. As the number of proteins is increased, the competition between attractive interactions and steric repulsions determines the stability and structure of the bound layer. The theory predicts that the competition between these two forces leads to a phase separation at higher protein concentrations. The point where this transition happens depends on both spacer length and protein surface coverage and is an important consideration for practical applications of these and other similar systems. If the goal is to maximize protein binding, it is favorable to be above the layer transition, as multiple layers can accommodate greater bound protein densities. On the other hand, if the goal is to use these bound proteins as a linker group to build more complex structures, such as when avidin or streptavidin serves as a linker between two biotinylated polymers or proteins, the optimum is to be below the layer transition such that all bound linker proteins are available for further binding.

- Direct Growth of ZnO Nanocrystals onto the Surface of Porous TiO<sub>2</sub> Nanotube Arrays for Highly Efficient and Recyclable Photocatalysts

Yang, H. Y.; Yu, S. F.; Lau, S. P.; Zhang, X.; Sun, D. D.; Jun, G. *Small* **2009**, *5*, 2260-2264.

Abstract:

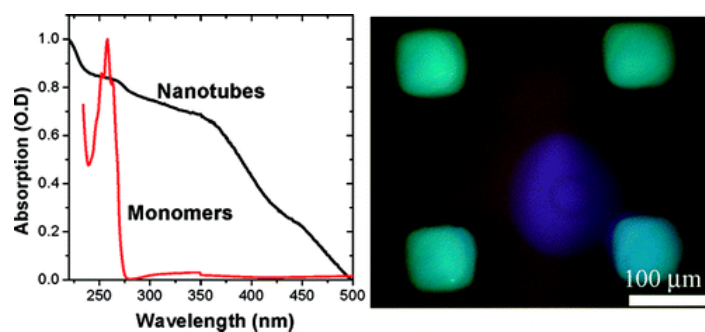


ZnO nanocrystal-coated, vertically oriented, porous TiO<sub>2</sub> nanotube arrays (see image) are used as efficient and low-cost photocatalysts. The exposed surface area and contact area are maximized to achieve high-efficiency photocatalytic decomposition via a heterojunction effect. The configuration of vertically aligned nanotube arrays also allows the diffusion of reactants through multiple pathways to enhance light harvest

- Blue Luminescence Based on Quantum Confinement at Peptide Nanotubes

Amdursky, N.; Molotskii, M.; Aronov, D.; Adler-Abramovich, L.; Gazit, E.; Rosenman, G. *Nano Lett.* **2009**, *9*, 3111–3115.

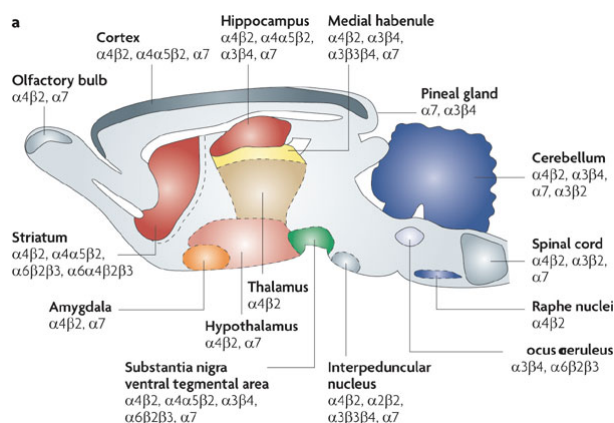
Abstract:



We report on observation of photoluminescence (PL) in blue and UV regions of exciton origin in bioinspired material—peptide nanotubes (PNTs). Steplike optical absorption and PL measurements have allowed finding quantum confined (QC) phenomenon in PNTs. The estimations show that QC in these nanotubes occurs due to a crystalline structure of subnanometer scale dimension formed under the self-assembly process. Our new findings pave the way for the integration of PNT in a new generation of optical devices. A blue PL array of a PNT-patterned device is demonstrated.

- Nicotinic receptors: allosteric transitions and therapeutic targets in the nervous system  
Taly, A.; Corringer, P.-J.; Guedin, D.; Lestage, P.; Changeux, J.-P. *Nature Reviews Drug Discovery* **2009**, *8*, 733-750.

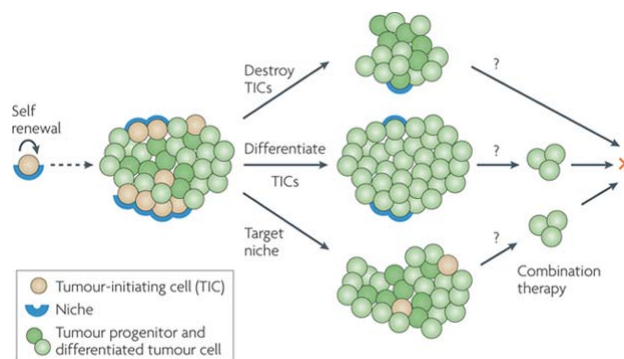
Abstract:



Nicotinic receptors — a family of ligand-gated ion channels that mediate the effects of the neurotransmitter acetylcholine — are among the most well understood allosteric membrane proteins from a structural and functional perspective. There is also considerable interest in modulating nicotinic receptors to treat nervous-system disorders such as Alzheimer's disease, schizophrenia, depression, attention deficit hyperactivity disorder and tobacco addiction. This article describes both recent advances in our understanding of the assembly, activity and conformational transitions of nicotinic receptors, as well as developments in the therapeutic application of nicotinic receptor ligands, with the aim of aiding novel drug discovery by bridging the gap between these two rapidly developing fields.

- Tumour-initiating cells: challenges and opportunities for anticancer drug discovery  
Zhou, B.-B. Z.; Zhang, H.; Damelin, M.; Geles, K. G.; Grindley, J. C.; Dirks, P. B. *Nature Reviews Drug Discovery* **2009**, *8*, 806-823.

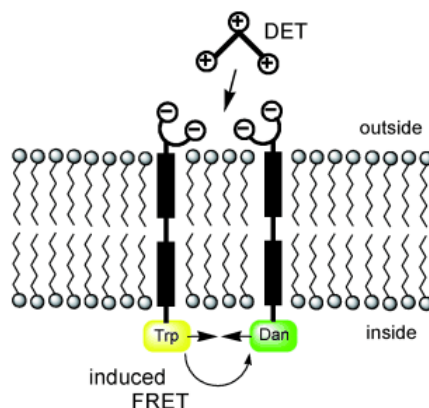
Abstract:



The hypothesis that cancer is driven by tumour-initiating cells (popularly known as cancer stem cells) has recently attracted a great deal of attention, owing to the promise of a novel cellular target for the treatment of haematopoietic and solid malignancies. Furthermore, it seems that tumour-initiating cells might be resistant to many conventional cancer therapies, which might explain the limitations of these agents in curing human malignancies. Although much work is still needed to identify and characterize tumour-initiating cells, efforts are now being directed towards identifying therapeutic strategies that could target these cells. This Review considers recent advances in the cancer stem cell field, focusing on the challenges and opportunities for anticancer drug discovery.

- Entirely Artificial Signal Transduction with a Primary Messenger  
Bernitzki, K.; Schrader, T. *Angew. Chem. Int. Ed.* **2009**, *48*, 8001–8005.

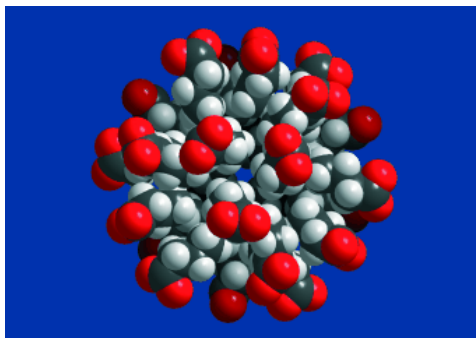
Abstract:



**I saw the sign:** An artificial system allows messenger-induced transmembrane signaling. External addition of a primary messenger molecule (DET, see picture) leads to formation of a heterodimeric complex of transmembrane units bearing tryptophan-dansyl (Trp-Dan) donor-acceptor pairs, which in turn stimulates a strong FRET on the opposite side of the membrane.

- A Spherical 24Butyrate Aggregate with a Hydrophobic Cavity in a Capsule with Flexible Pores: Confinement Effects and Uptake–Release Equilibria at Elevated Temperatures  
Schäffer, C.; Bögge, H.; Merca, A.; Weinstock, I. A.; Rehder, D.; Haupt, E. T. K.; Müller, A. *Angew. Chem. Int. Ed.* **2009**, *48*, 8051–8056.

Abstract:



**Forced interaction:** The encapsulation of a large assembly of organic species - the 24 butyrate unit, which exhibits a remarkable central spherical hydrophobic cavity spanned by 72 H atoms - in a porous capsule (see picture) leads to interesting interactions between the butyrates under the confined conditions. The quarantine for the guests is lifted upon temperature increase: guests can easily leave and return.